

Are your MRI contrast agents cost-effective?

Learn more about generic Gadolinium-Based Contrast Agents.



**FRESENIUS
KABI**

caring for life

AJNR

**Non-heme mechanisms for T1 shortening:
pathologic, CT, and MR elucidation.**

O B Boyko, P C Burger, J D Shelburne and P Ingram

AJNR Am J Neuroradiol 1992, 13 (5) 1439-1445

<http://www.ajnr.org/content/13/5/1439>

This information is current as
of April 3, 2024.

Non-Heme Mechanisms for T1 Shortening: Pathologic, CT, and MR Elucidation

Orest B. Boyko,^{1,4} Peter C. Burger,² John D. Shelburne,² and Peter Ingram³

PURPOSE: To further elucidate the nonparamagnetic effects of T1-relaxation mechanisms in MR imaging. **PATIENTS AND METHODS:** In 12 patients with lesions having hyperintense signal on T1-weighted spin-echo MR, findings were correlated with autopsy/surgical biopsy in seven cases and/or noncontrast CT scans in 10 cases. **RESULTS:** Eight of the 10 CT scans demonstrated hyperattenuation in the lesions, indicating mineralization, which correlated with the areas of hyperintense signal on MR. Histologic characterization of the mineralization was accomplished in three cases using four stains; hematoxylineosin, alizarin red S, von Kossa stains for calcium and Perls' iron. The areas of mineralization were homogeneously strongly positive with the calcium stains and only focally weakly positive with the Perls' iron stain. The mineralization was further characterized in all three cases as containing calcium and phosphorus using energy-dispersive x-ray analysis. Four of the 12 cases had either no correlating CT scans (two cases) or the CT showed no hyperattenuating properties to the lesions (two cases). In all four of these cases, microscopic examination showed that the gyriform configuration of the cortical hyperintense signal on T1-weighted images correlated with linear zones of nonhemorrhagic laminar necrosis (cerebral infarction). No mineralization, except for an occasional ferruginated neuron, could be demonstrated with the four histologic stains. Specimen MR imaging of formalin-fixed brain sections in one case demonstrated in vitro the gyriform hyperintense signal seen in vivo. **CONCLUSION:** Our studies describe and pathologically characterize two associations with T1 shortening in neuroimaging unrelated to the presence of heme: 1) calcification and 2) laminar necrosis in cerebral infarction.

Index terms: Magnetic resonance, tissue characterization; Radiologic-pathologic correlations

AJNR 13:1439-1445, Sep/Oct 1992

The advent of new neuroimaging modalities has been associated with different sensitivities for detecting pathologic tissue matrix: calcium with computed tomography (CT) (1) and blood products with magnetic resonance (MR) (2-5). Understanding the limitations of MR in characterizing lesions is partly dependent on the availability of direct pathologic correlation. As an example, intracranial calcification on T1-weighted spin-echo

MR imaging has been classically described as having hypointense or isointense signal relative to brain (6-9, 10, 11). Recent reports have been published concerning the association of intracranial calcium with hyperintense signal on T1-weighted images (12-16) but histologic correlation is available in only one case (14). In addition, a noncalcified and nonhemorrhagic hypercellular brain tumor has been associated with T1 shortening (17), suggesting cellular morphologic architecture can also affect the overall T1-relaxation properties of a tissue.

We provide further in vivo CT and MR and/or in vitro pathologic correlation for the association of diamagnetic mineral (calcium/phosphorus) and pathologic cellular architecture (infarct) with T1 shortening unrelated to any detectable paramagnetic effect from heme. Two pathologic entities (calcification and infarct) need to be added to the differential list of causes for hyperintense

Received July 24, 1991; accepted and revisions requested August 30; revision received December 5.

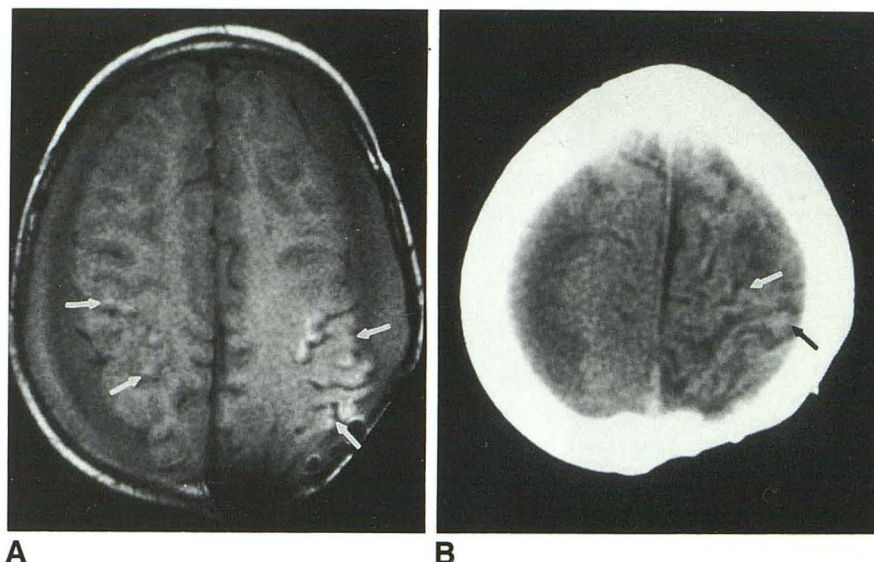
Presented at the 29th Annual Meeting of the ASNR, Washington, DC, June 9-14, 1991.

Departments of ¹ Radiology and ² Pathology, Duke University Medical Center, Durham, NC. ³ Research Triangle Institute, Research Triangle Park, NC.

⁴ Address reprint requests to Orest B. Boyko, MD, PhD, Box 3808, Department of Radiology, Duke University Medical Center, Durham, NC 27710.

AJNR 13:1439-1445, Sep/Oct 1992 0195-6108/92/1305-1439
© American Society of Neuroradiology

Fig. 1. Noncontrast T1-weighted MR image (A) shows cortically based hyperintense signal in both cerebral hemispheres (arrows) and bilateral isointense subdural fluid collections. Previous MR study did not show this hyperintense signal and follow-up MR 1 year later showed no resolution of the signal. Noncontrast CT scan showed that the areas of shortened T1 in A correlated with the presence of hyperattenuating mineralization in the left hemisphere (B, arrows) but mineralization could not be detected in the right hemisphere. The mineralization, presumed to be calcium, was secondary to radiation therapy.



signal (T1 shortening) on T1-weighted spin-echo MR imaging.

Subjects and Methods

Twelve cases of signal hyperintensity on T1-weighted spin-echo imaging comprise this report. Noncontrast CT scans were available in 10 patients. MR imaging parameters at 1.5 T included 256×128 or 256×192 matrix. T1-weighted parameters were 500–700/20/1–2 (TR/TE/excitations). Postmortem T1-weighted images were obtained at 500/20, 500/10, or 200/10.

Autopsy/surgical biopsy pathologic correlation was available in seven cases. Histologic stains used for detecting mineralization included hematoxylineosin (H & E), and alizarin red S (18) or von Kassa for calcium. Histologically identified mineralization was further characterized using energy-dispersive x-ray analysis (EDXA) in three cases (19, 20).

Briefly, EDXA was performed using an ETEC scanning electron microscope equipped with a Kevex 5100 energy-dispersive x-ray analyzer (Kevex Corp., Burlingame, CA) with a 30×30 mm Si (Li) detector (19, 20). A working distance of 16 mm was used in the fast raster mode. The tilt was 30° and a 20 kV accelerating voltage was used. The condenser current was 2.15 A and the vertical scale was 8,000 counts. Additional localization and conventional electron microscopic image generation was available by converting to backscattered electron imaging capabilities. Spectral peaks could thus be definitely acquired in areas with or without mineralization. Tissue specimens to be analyzed by EDXA were processed from routine histologic paraffin blocks, deparaffinized with xylol, and mounted on a carbon stub and lightly carbon coated.

Results

Our 12 cases of hyperintense lesions on T1-weighted MR imaging were subdivided based on

the CT findings. Eight cases had hyperattenuating CT properties in the areas of hyperintense MR signal, indicating the lesions were mineralized. The five lesions with only CT correlation were a peripherally calcified intracranial aneurysm, calcified optic nerve glioma, basilar artery calcification, an unbiopsied calcified area of an oligodendroglioma, and gray-white junction mineralization from radiation change (Fig. 1).

Histologic correlation was available for the other three cases of hyperattenuating CT lesions. The pathologic diagnoses were bilateral basal ganglia mineralization in a pediatric AIDS patient (Fig. 2), oligodendroglioma (Fig. 3), and cranio-pharyngioma. The mineralization detected by CT in all three lesions (Fig. 2B) was homogeneously strongly positive for calcium by H & E, alizarin red S, and von Kassa stains (Figs. 2C and 3B). There was very inhomogeneous focal weak positivity with Perls' iron stain in the areas of calcification in two cases. No hemorrhage could be identified.

EDXA spot probes further identified in all three cases that the major component of the mineralization seen on the backscattered positive electron microscope images (Fig. 3C) was calcium and phosphorous (Fig. 2D) that was not present in the backscattered negative areas (Fig. 2E).

In four of the 12 cases, correlative CT scans were either not available (two cases) or demonstrated no associated hyperattenuation or mineralization (two cases) in the lesions. Surgical biopsy or autopsy correlation in all four cases showed nonhemorrhagic cerebral infarction. In all four cases, the T1-weighted MR images demonstrated

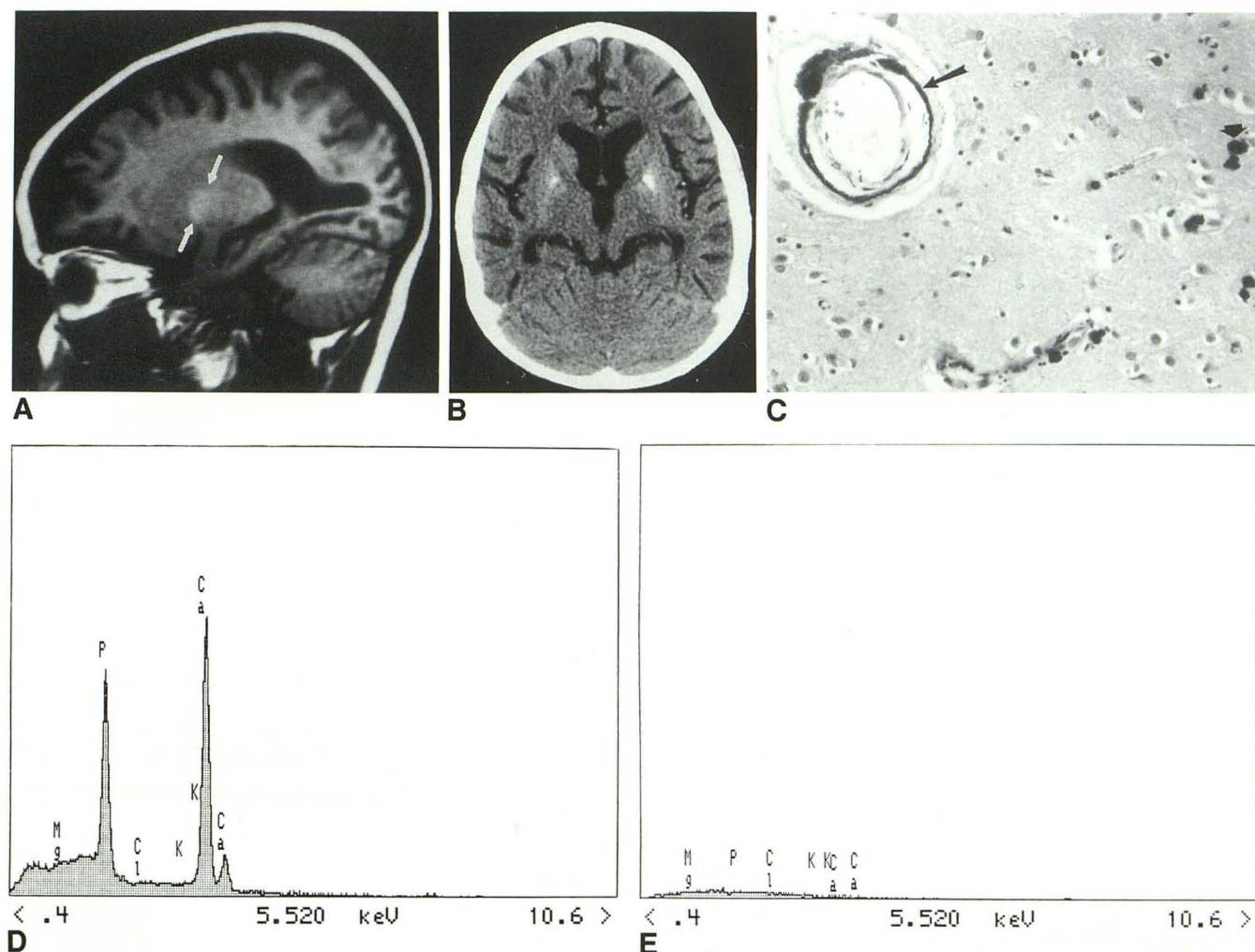


Fig. 2. A, Sagittal T1-weighted noncontrast MR image in a pediatric AIDS patient shows hyperintense signal in the basal ganglia (arrows).

B, Axial noncontrast CT scan shows cerebral atrophy and that the bilateral basal ganglia hyperintense signal are associated with hyperattenuating mineralization (probable calcium).

C, H & E (100X) photomicrograph of autopsy material shows that the mineralization seen on CT scan (B) is perivascular (arrow) and intraparenchymal (arrowhead) calcium that was also confirmed by alizarin red S and von Kassa stains. Several of the calcium deposits stained weakly for ferric iron by the Perls' stain.

D, EDXA x-ray spectra obtained from spot probes shows the mineralization seen on CT (B) and histologically (C) to be comprised predominantly of calcium and phosphorus. The iron detected by the Perls' stain could not be detected by EDXA, suggesting either a sampling error or most likely the fact that the Perls' iron stain is more sensitive than EDXA in the detection of iron.

E, Control EDXA x-ray spectra obtained from spot probes where there was no mineralization shows no tissue background for calcium or phosphorus.

an evolution of cortically based linear hyperintense signal conforming to the gyri (Figs. 4A–4C) that over time (months) became less intense (Fig. 4C). Histologic correlation showed cortical laminar necrosis (Fig. 4D). The gyriform pattern of T1 shortening could be identified on T1-weighted MR imaging of formalin-fixed brain sections (Fig. 5A). Histologic correlation of these hyperintense foci demonstrated cortical-based linear zones of laminar necrosis without evidence for hemorrhage (Fig. 5B). These areas did not stain positive

for minerals with either H & E, alizarin red S, or von Kassa stains. Perls' iron showed an occasional ferruginated neuron. One case had neuronal pigment incontinence as a hallmark of ischemia/infarct in the cortical gray matter.

Discussion

Hyperintense signal on T1-weighted images has been classically associated with intra- or extracellular methemoglobin (2–5), such as in hem-

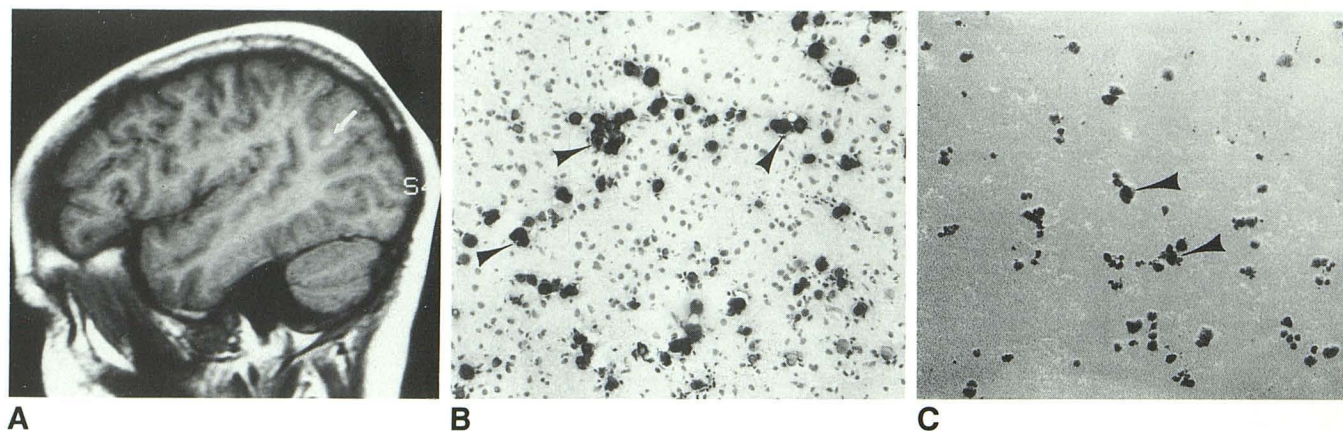


Fig. 3. A, Sagittal T1-weighted noncontrast MR image in an adolescent with long-standing seizures shows a hyperintense subcortical lesion (arrow).

B, Histologic section (H & E, 170X) shows a diffusely mineralized (arrowheads) hypercellular tumor (oligodendroglioma). Alizarin red S and von Kassa stains further confirmed the presence of calcium in the mineralized portions of the tumor.

C, Backscattered electron microscope image (150X) using the scanning electron microscope mode of the EDXA instrument shows backscatter positive extracellular mineralization (arrowheads). EDXA x-ray spectrum showed the mineralization to be comprised of calcium and phosphorus.

orrhagic infarcts (21), mucin (22), high protein concentration (23, 24) or lipid/cholesterol (22, 25). Our pathologic, CT, and MR correlation would argue for including calcium and nonhemorrhagic cerebral infarction in the consideration of pathologic processes, accounting for the T1 shortening properties of tissues. Realization of such causes for T1 shortening does influence clinical interpretation and differential diagnosis.

Calcium's effect on the signal intensity in spin-echo MR imaging has been initially reported to be variable; ranging from hypointense to signal dampening to imperceptible (6–8, 9–11). Recently, however, the association of high signal intensity on T1-weighted images with hyperattenuating regions on CT scan, presumed to be calcium, have been reported (12, 13, 15, 16). In none of these cases was tissue available to confirm calcium histologically.

One case has been reported where hyperintense signal was present on T1-weighted images (14) and calcium was demonstrated histologically. In that case report however, the CT scan did not have Hounsfield units indicative of calcium, although the lesion was hyperdense on noncontrast scans.

Henkelman and coworkers recently reported their findings in 10 patients with hyperintense signal on T1-weighted images (16). The lesions in all 10 patients were hyperattenuating on CT scan. In vitro correlation using diamagnetic substances (calcium hydroxylapatite and calcium carbonate) were shown to affect the T1 relaxation

of water and the degree of T1 shortening was directly related to the surface area of the calcium crystals (16). The findings of calcium phosphate causing T1 shortening in test tube phantom studies has also been previously published by Dell et al (13), in agreement with the findings of Henkelman et al (16) on the effect by diamagnetic substances on T1 relaxation. We provide further extension of the work of both groups by providing histologic confirmation by EDXA that the mineralization identified on CT scans in areas demonstrating T1 shortening is predominantly calcium and phosphorous.

Henkelman and coworkers (16) have elegantly summarized in their paper the previous literature concerning the effects of calcium on MR signal intensity. Previous work on the NMR signal effects of "inert" or diamagnetic particles has conclusively demonstrated their T1 shortening ability (26–28). In addition, phantom work using simulated calcified lung nodules (29) and powdered trabecular bone (30) has also shown an association of calcium with an increase in T1 relaxivity.

A hypothesis to explain this surface phenomena of enhanced relaxivity by calcium has been presented (16), similar to that for large proteins, where the rotational and translational frequencies of the bound layer of water nearest the calcium crystal surface are closer to the Larmor frequency than water molecules distant to the surface. The water molecules closest to the surface thus relax more quickly (16).

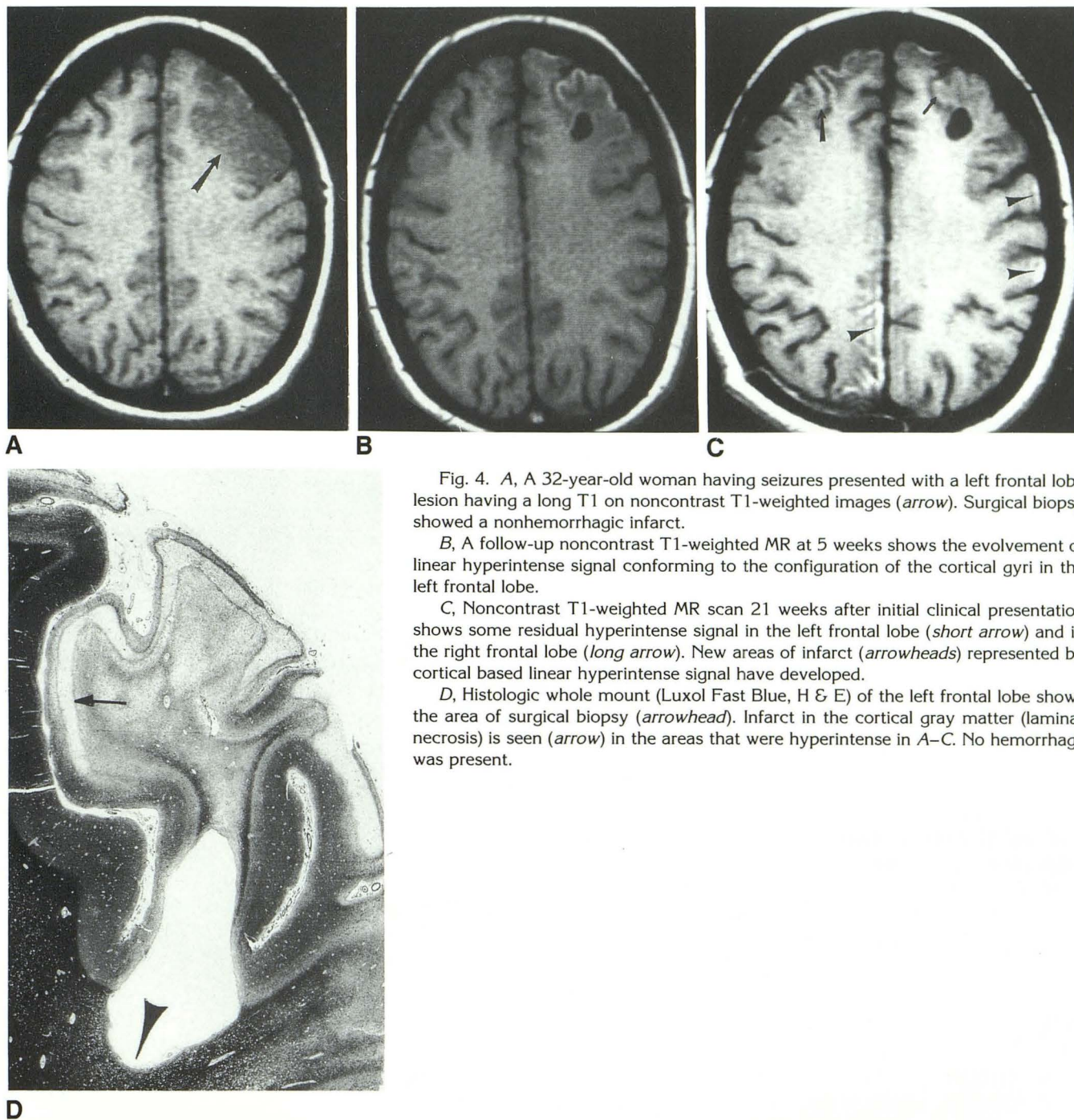


Fig. 4. A, A 32-year-old woman having seizures presented with a left frontal lobe lesion having a long T1 on noncontrast T1-weighted images (arrow). Surgical biopsy showed a nonhemorrhagic infarct.

B, A follow-up noncontrast T1-weighted MR at 5 weeks shows the evolution of linear hyperintense signal conforming to the configuration of the cortical gyri in the left frontal lobe.

C, Noncontrast T1-weighted MR scan 21 weeks after initial clinical presentation shows some residual hyperintense signal in the left frontal lobe (short arrow) and in the right frontal lobe (long arrow). New areas of infarct (arrowheads) represented by cortical based linear hyperintense signal have developed.

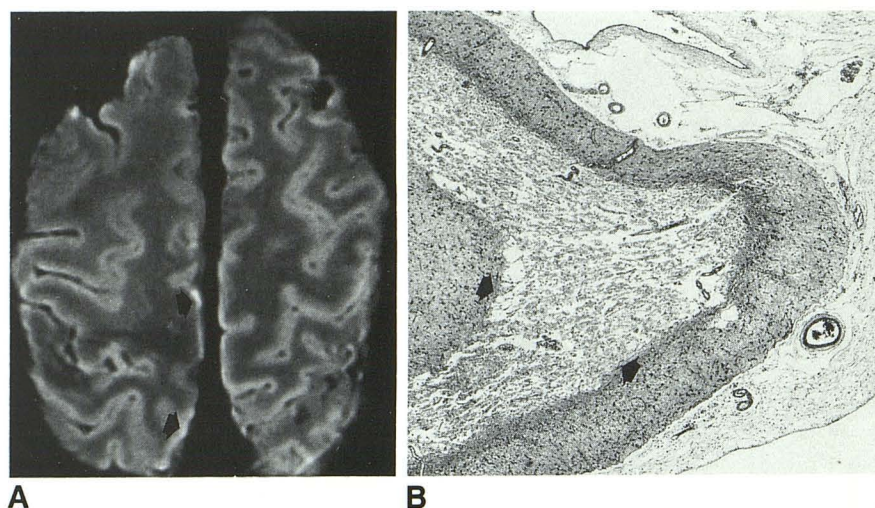
D, Histologic whole mount (Luxol Fast Blue, H & E) of the left frontal lobe shows the area of surgical biopsy (arrowhead). Infarct in the cortical gray matter (laminar necrosis) is seen (arrow) in the areas that were hyperintense in A–C. No hemorrhage was present.

It is very doubtful that the very minimal presence of iron we identified in some of the mineralized foci has a contribution to the T1 relaxation mechanism observed on the clinical images since iron does not affect T1 relaxation (31) unless it is in its free form (16, 32). We, of course, cannot exclude the fact that some paramagnetic elements that may have been chelated to the calcium could have been "washed out" during the normal tissue processing of the formalin-fixed

tissue. Previous EDXA microprobe work (33) in cases of Fahr disease reported the presence of calcium, zinc, aluminum, magnesium, phosphorous, iron, chloride, sulfur, and potassium.

The mechanism for the increased T1 relaxation of the cerebral infarcts that can dissipate over months is less apparent. The finding of a gyriform configuration of hyperintense signal on T1-weighted images has been previously reported in six of 46 stroke patients (21). There was no

Fig. 5. Postmortem T1-weighted specimen MR of formalin-fixed brain sections of the same patient as in Figure 4 shows the presence of gyriform areas of hyperintense signal (A, arrowheads) seen on in vivo imaging conforming to areas of nonhemorrhagic cortical laminar necrosis (B, arrowheads) histologically.



pathologic correlation available and the suggestion that the areas of high signal were due to hemorrhage is not substantiated by the pathologic correlation in our four cases of cerebral infarct. We could not demonstrate any calcium, however, either by special stains or CT. Thus, we cannot exclude the fact that again it is possible that some paramagnetic moiety or more soluble calcium may have "washed out" during histologic processing from the area of infarct since the presence of calcium in areas of hypoxic ischemia has been previously described (34). In addition, T1 relaxation from denatured proteins and cellular components in the areas of infarct could be postulated to contribute to the T1 shortening we have observed similar to the effect by high protein (protein hydration layer effect).

Establishing an association of chronic infarction with hyperintensity on T1-weighted images does raise the possibility of this actually being the major effect in two of our cases with mineralization. The autopsied case of AIDS calcification (Fig. 2) had no histologic evidence for basal ganglia ischemia/infarction serving as a nidus for the dystrophic calcification. The case of radiation change (Fig. 1) had no histologic correlation but the stability of the MR findings on follow-up scans and the lack of contrast enhancement on both CT and MR would tend to exclude radiation necrosis. However, ischemic change from radiation effect accounting for the T1 shortening cannot be excluded. Ischemia may well be the likely explanation accounting for the T1 shortening in the right hemisphere since no mineral was detected on CT and the sensitivity of CT over MR in detecting calcium is clearly established.

Interestingly, lesions with hypercellularity and a high cytoplasmic/nuclear ratio have been reported to be associated with an enhanced T1 relaxation mechanism (14, 17, 35) that may also represent a protein hydration layer effect (17).

Calcium deposition and cerebral infarcts are pathologic processes that can both be associated with T1 shortening that does not seem to be related to any paramagnetic effects from heme/hemorrhage. In the differential diagnosis of lesions demonstrating short T1 relaxation properties consideration should be made of including cerebral infarct or diamagnetic mineral such as calcium along with intra- and extracellular methemoglobin/hemorrhage, mucin, high protein concentration, or lipid/cholesterol. Further strict pathologic/radiologic correlation will uncover other new associated relaxation properties of pathologic lesions.

Acknowledgments

Special thanks to Drs. Mark Henkelman and Walter Kucharczyk for their discussions of the phenomena of T1 shortening by calcium and for their review of this manuscript.

References

1. Norman D, Diamon C, Boyd D. Relative detectability of intracranial calcifications on computer tomography and skull radiography. *J Comput Assist Tomogr* 1978;2:62-64
2. Sipponen JT, Sepponen RE, Sivula A. Nuclear magnetic resonance (NMR) imaging of intracerebral hemorrhage in the acute and resolving phases. *J Comput Assist Tomogr* 1983;7:954-959
3. Bradley WG, Schmidt PG. Effect of methemoglobin formation on the MR appearance of subarachnoid hemorrhage. *Radiology* 1985;156:99-103

4. Gomori JM, Grossman RI, Goldberg HI, et al. Intracranial hematomas, imaging by high-field MR. *Radiology* 1985;157:87-93
5. Gomori JM, Grossman RI, Hackney DB, Goldberg HI, Zimmerman RA, Bilaniuk LT. Variable appearances of subacute intracranial hematomas on high-field spin-echo MR. *AJNR* 1987;8:1019-1026
6. Holland BA, Kucharczyk W, Brant-Zawadzki M, Norman D, Haas DK, Harper PS. MR imaging of calcified intracranial lesions. *Radiology* 1985;157:353-356
7. Oot RF, New PF, Pile-Spellman J, Rosen BR, Shoukimas GM, Davis KR. The detection of intracranial calcifications by MR. *AJNR* 1986;7:801-809
8. Brant-Zawadzki M, Davis PL, Crooks LE, et al. NMR demonstration of cerebral abnormalities: comparison with CT. *AJNR* 1983;4:1013-1026
9. Kjos BO, Brant-Zawadzki M, Kucharczyk W, Kelly WM, Norman D, Newton TH. Cystic intracranial lesions: magnetic resonance imaging. *Radiology* 1985;155:363-369
10. Zimmerman RD, Fleming CA, Saint-Louis LA, Manning JJ, Deck MDF. Magnetic resonance imaging of meningiomas. *AJNR* 1985;6:149-157
11. Atlas SW, Grossman RI, Hackney DB, et al. Calcified intracranial lesions: detection with gradient-echo-acquisition rapid MR imaging. *AJNR* 1988;9:253-259
12. Chatillon J d'Ade, Billy A, Dormant D, et al. Calcifications idiopathiques des noyaux gris centraux (maladie de Fahr): apport de l'imagerie par resonance magnetique. *Presse Med* 1988;17:1760
13. Dell LA, Brown MS, Orrison WW, Eckel CG, Matwiyoff NA. Physiologic intracranial calcification with hyperintensity on MR imaging: case report and experimental model. *AJNR* 1988;9:1145-1148
14. Tien RD, Hesselink JR, Duberg A. Rare subependymal giant-cell astrocytoma in a neonate with tuberous sclerosis. *AJNR* 1990;11:1251-1252
15. Araki Y, Furukawa T, Tsuda K, et al. High field MR imaging of the brain in pseudohypoparathyroidism. *Neuroradiology* 1990;32:325-327
16. Henkelman RM, Watts JF, Kucharczyk W. High signal intensity in MR images of calcified brain tissue. *Radiology* 1991;179:199-206
17. Abe K, Hasegawa H, Kobayashi Y, et al. A gemistocytic astrocytoma demonstrated high intensity on MR images: protein hydration layer. *Neuroradiology* 1990;32:166-167
18. Proia AD, Brinn NT. Identification of calcium oxalate crystals using alizarin red S stain. *Arch Pathol Lab Med* 1985;109:186-189
19. Ingram P, Shelburne JD, Roggli VI. *Microprobe analysis in medicine*. New York: Hemisphere, 1989
20. Baker D, Kupke KG, Ingram P. Microprobe analysis in human pathology. *Electron Microsc* 1985;2:659-680
21. Nabatame H, Fujimoto N, Nakamura K, et al. High intensity areas on noncontrast T1-weighted MR images in cerebral infarction. *J Comput Assist Tomogr* 1990;14:521-526
22. Maeder PP, Holtas SL, Basibuyuk LN, et al. Colloid cyst of the third ventricle: correlation of MR and CT findings with histology and chemical analysis. *AJNR* 1990;11:575-581
23. Tien RD, Barkovich AJ, Edwards MSB. MR imaging of pineal tumors. *AJNR* 1990;11:557-581
24. Som PM, Dillon WP, Fullerton GD, et al. Chronically obstructed sinonasal secretion: observations on T1 and T2 shortening. *Radiology* 1989;172:515-520
25. Horowitz BL, Chari MV, Reese J, Bryan RN. MR of intracranial epidermoid tumors: correlation of in vivo imaging with in vitro ¹³C spectroscopy. *AJNR* 1990;11:299-302
26. Glasel JA, Lee KH. On the interpretation of water nuclear magnetic resonance relaxation times in heterogeneous systems. *J Am Chem Soc* 1974;96:970-978
27. Woessner DE. An NMR investigation into the range of the surface effect on the rotation of water molecules. *J Magn Reson* 1980;39:297-308
28. Hanus F, Gillis P. Relaxation of water absorbed on the surface of silica powder. *J Magn Reson* 1984;59:437-445
29. Gamsu G, De Geer G, Cann C, et al. A preliminary study of MRI quantification of simulated calcified pulmonary nodules. *Invest Radiol* 1987;22:853-858
30. Davis CA, Genant HK, Dunham JS. The effects of bone on proton NMR relaxation times of surrounding liquids. *Invest Radiol* 1986;21:472-477
31. Drayer BP, Burger P, Darwin R, et al. Magnetic resonance imaging of brain iron. *AJNR* 1986;7:373-380
32. Hardy PA, Henkelman RM. Transverse relaxation rate enhancement caused by magnetic particulates. *Magn Reson Imaging* 1989;7:265-275
33. Duckett S, Galle P, Escourolle R, Poirier J, Hauw J. Presence of zinc aluminum, magnesium in striopallidodentate (SPD) calcifications (Fahr's Disease): electron probe study. *Acta Neuropathol (Berl)* 1977;38:7-10
34. Ansari MQ, Chincanchan CA, Armstrong DL. Brain calcification in hypoxic-ischemic lesions: an autopsy review. *Pediatr Neurol* 1990;6:94-101
35. Barakos JA, Brown JJ, Brescia RJ, Higgins CB. High signal intensity lesions of the chest in MR imaging. *J Comput Assist Tomogr* 1989;13:797-802